

Electronic Supplementary Information

Experimental section

Materials characterization

The morphology of the catalysts was analyzed by various instruments, including scanning electron microscopy (SEM, ZEISS GeminiSEM 500), transmission electron microscopy (TEM, TalosS-FEG), high-angle annular dark-field scanning transmission electron microscopy (HAADF-STEM, TalosS-FEG), selected area electron diffraction (SEAD, TalosS-FEG), high-resolution transmission electron microscopy (HRTEM, TalosS-FEG), and energy dispersive X-ray spectroscopy (EDX). The thickness of the metallene was measured by Atomic force microscopy (AFM, MFP-3D Infinity, Asylum Research). Furthermore, crystalline structure, surface chemical composition and valence state of the catalysts were examined with X-ray powder diffraction (XRD, Ultima IV, Rigaku) and X-ray photoelectron spectroscopy (XPS, K-Alpha, Thermo Scientific.). The ultraviolet-visible (UV-vis) absorbance of the anodic electrolyte was measured using a Beijing Pugin General T6 New Century spectrophotometer.

Electrochemical investigation

Electrochemical measurements were conducted in a standard three-electrode cell system with a CHI 660E instrument (CH Instruments). To prepare the catalyst ink, the as-prepared SP-Rhlene was dissolved in 1 mL mixed solution (volume ratio, 0.5% Nafion: ethanol: water = 1: 2: 7). The HER polarization curves were conducted in 1 M KOH solution. The glassy carbon electrode (GCE) coated with the prepared catalyst, a saturated Hg/HgO and a graphite rod were used as the working electrode, reference

electrode, and counter electrode, respectively. To prepare the catalyst ink, the as-prepared SP-RhIene (2 mg) was dissolved in 1 mL mixed solution (composition and proportion as above). The GCE was modified with ink (5 μ L) and dried at 60 $^{\circ}$ C. The catalyst ink for SOR and SOR-HER measurements were prepared by ultrasonically dissolving 5 mg sample in 1 mL mixed solution. For the SOR tests, the carbon paper (CP) with 200 μ L catalyst ink was served as the working electrode in 1 M KOH with 4 M Na₂S. The HER-SOR system was tested in an H-type electrolytic cell with CP as the cathode and anode in 1 M KOH with 4 M Na₂S. The electrochemical impedance spectroscopy (EIS) curves were obtained over a frequency range from 100 kHz to 0.1 Hz.

The catalysts' electrochemical active surface areas (ECSAs) were determined by calculating the peak areas from the cyclic voltammogram (CV) curves, which were obtained by performing 10 cycles of CV in a 1 M KOH solution, at a scan rate of 50 mV s⁻¹. The ECSAs of different catalysts were obtained by using the equation below:

$$\text{ECSA} = Q/(mC)$$

Q is the charge associated with the peak, m is the loading of Rh metals, C (425 μ C cm⁻²) is the needed for the reduction of Rh monolayer on the catalyst.

The Faraday efficiency (FE) was obtained by calculating the actual and theoretical values of the cathode and anode. In a customized H-type cell, separated by Nafion 211 membrane, CP was used as cathode and anode, and modified with 1 mg cm⁻² sample.

The FE was calculated by the following formula.

$$FE_s(\%) = \frac{n \times N \times F}{j \times t} \times 100\%$$

Where n represents the molar amount that generates a specific product, N represents the number of electrons that have undergone a specific reaction transfer, F represents the Faraday constant (96485 C mol^{-1}), j denotes the total current density, and t is the electrolysis time.

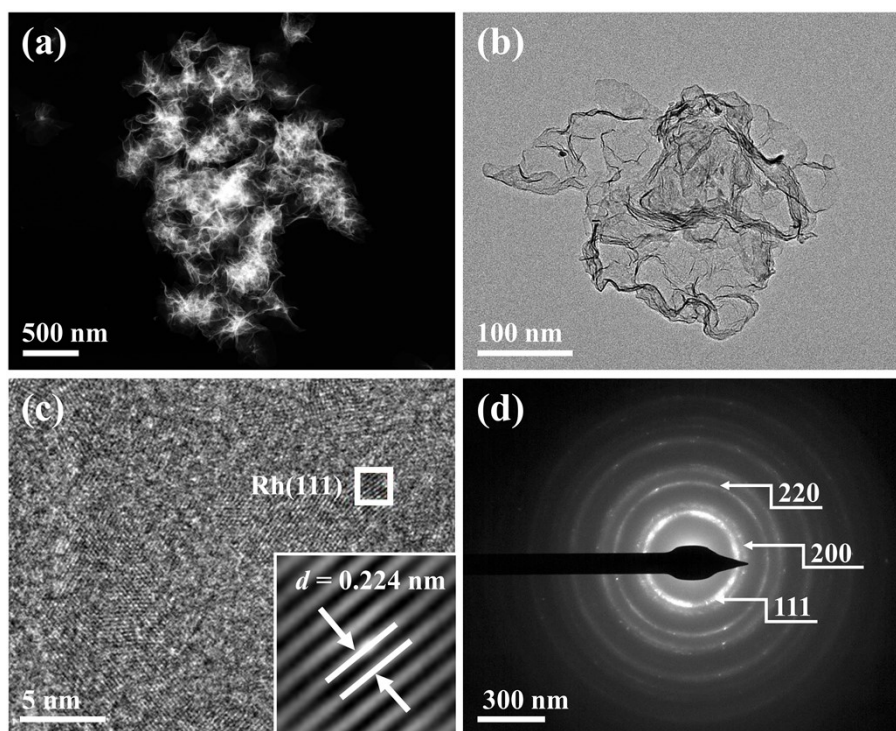


Fig. S1 (a) HAADF-STEM image and (b) TEM image of the Rhlene. (c) HRTEM image of the Rhlene and corresponding Fourier-filtered lattice fringe image. (d) The SEAD image of Rhlene.

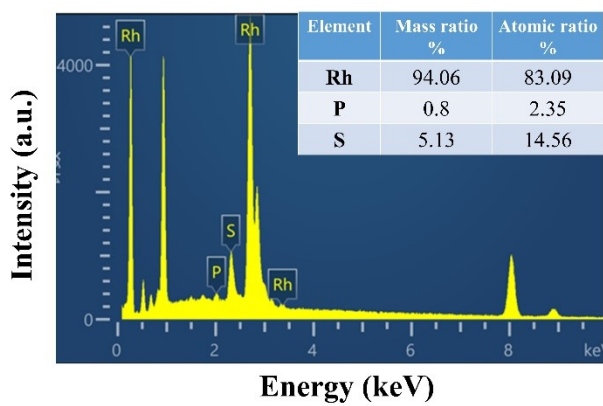


Fig. S2 EDX spectrum of the SP-Rhene.

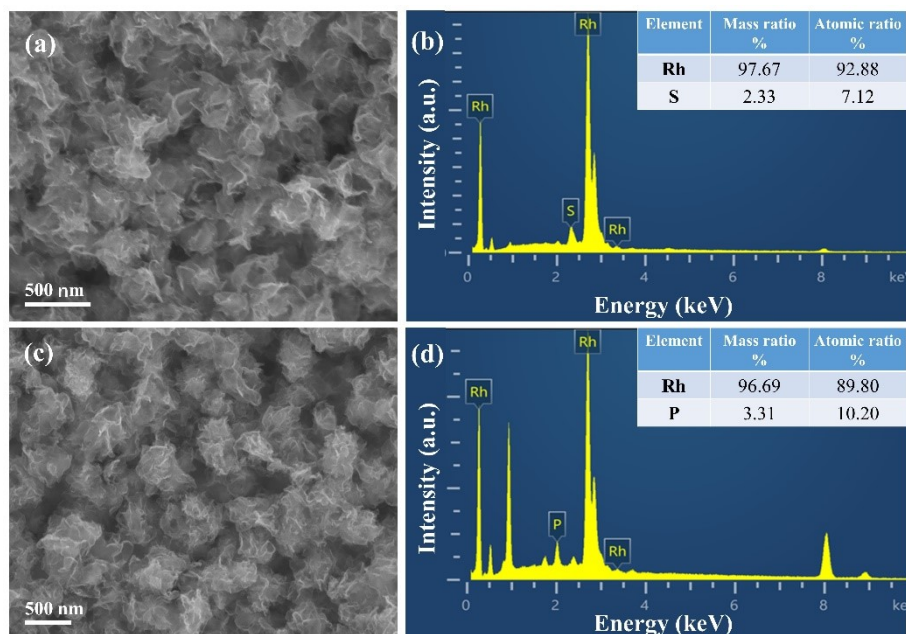


Fig. S3 SEM images and EDX spectra of the (a, b) S-Rhylene and (c, d) P-Rhylene.

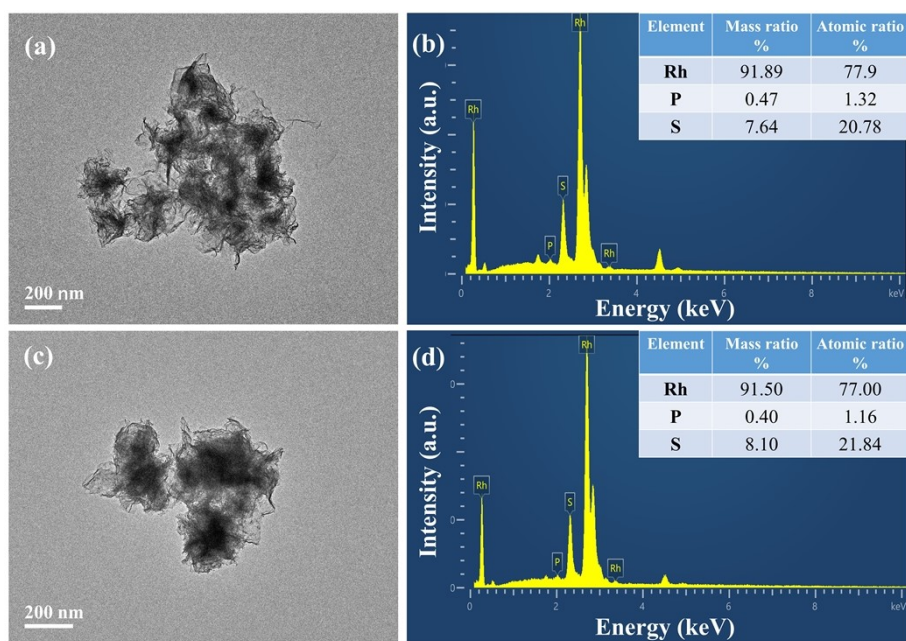


Fig. S4 TEM images and EDX spectra of the (a, b) SP-Rhylene (4 mg) and (c, d) SP-Rhylene (8 mg).

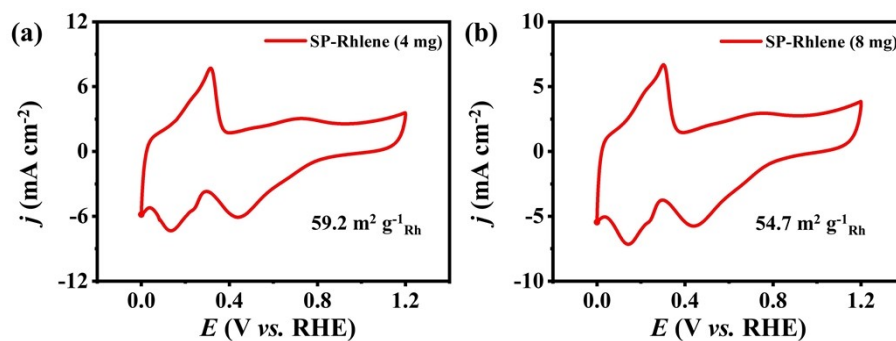


Fig. S5 CV curves and ECSAs of various SP-Rhylene samples with different TPS adding amounts: (a) 4 mg TPS, (b) 8 mg TPS.

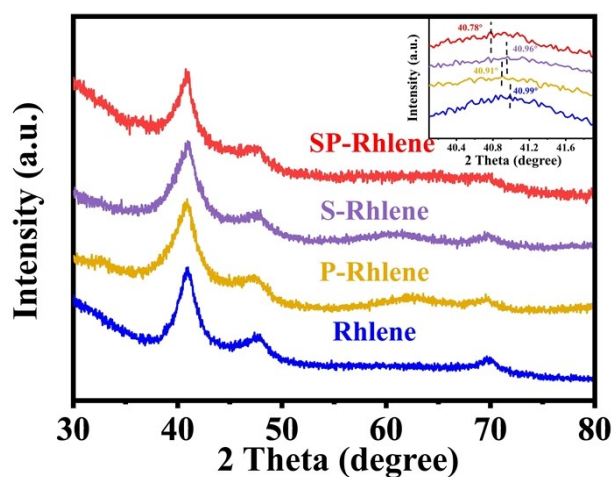


Fig. S6 XRD patterns of the SP-Rhylene, S-Rhylene, P-Rhylene and Rhylene.

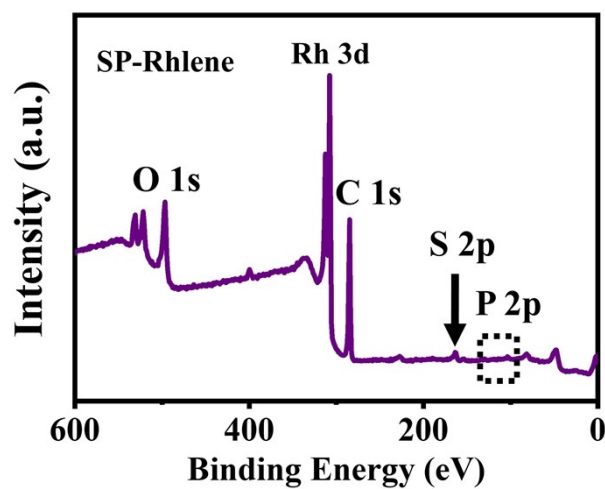


Fig. S7 The XPS survey spectrum of the SP-Rhylene.

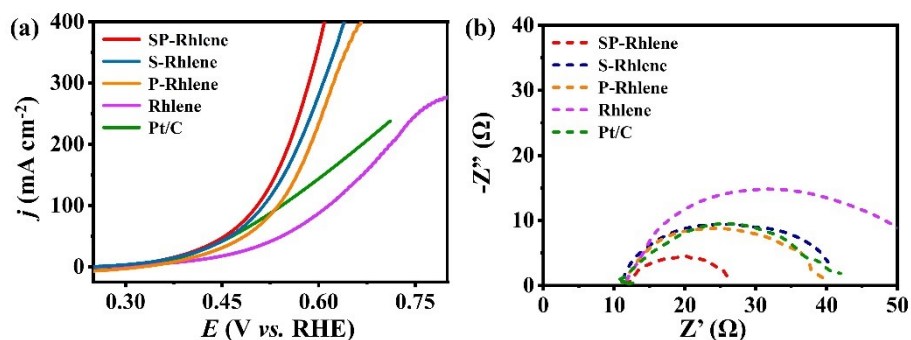


Fig. S8 (a) SOR polarization curves of SP-Rhylene and contrast samples. (b) Nyquist plots for SP-Rhylene and contrast samples in 1 M KOH containing 4 M Na₂S.

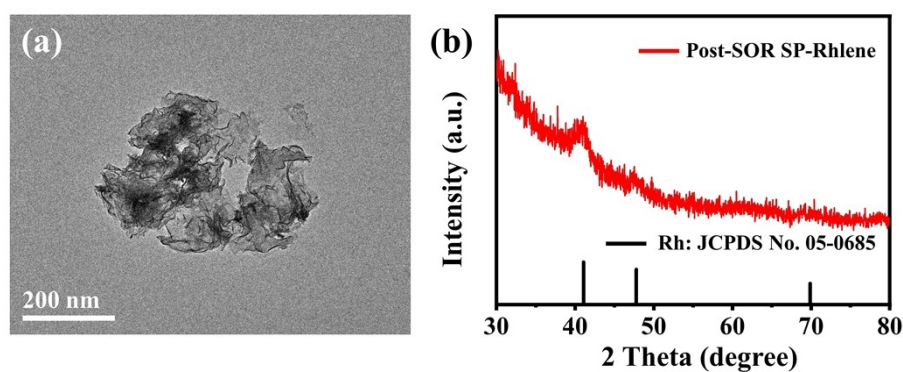


Fig. S9 (a) TEM image and (b) XRD pattern of the SP-Rhylene after long-term SOR stability testing.

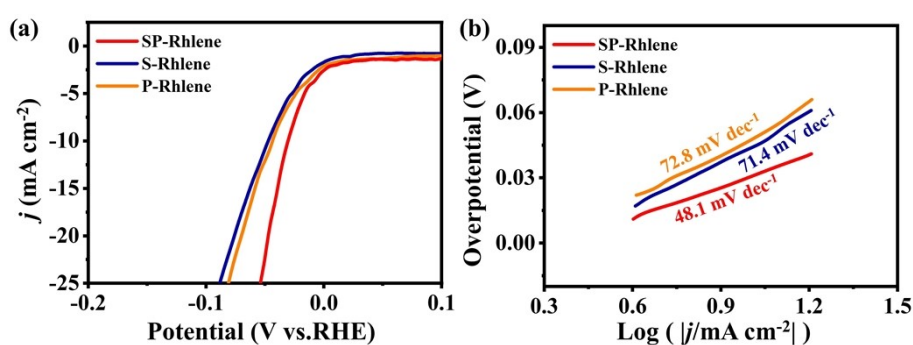


Fig. S10 (a) HER polarization curves and (b) Tafel plots for SP-Rhylene, S-Rhylene, and P-Rhylene in 1 M KOH solution.

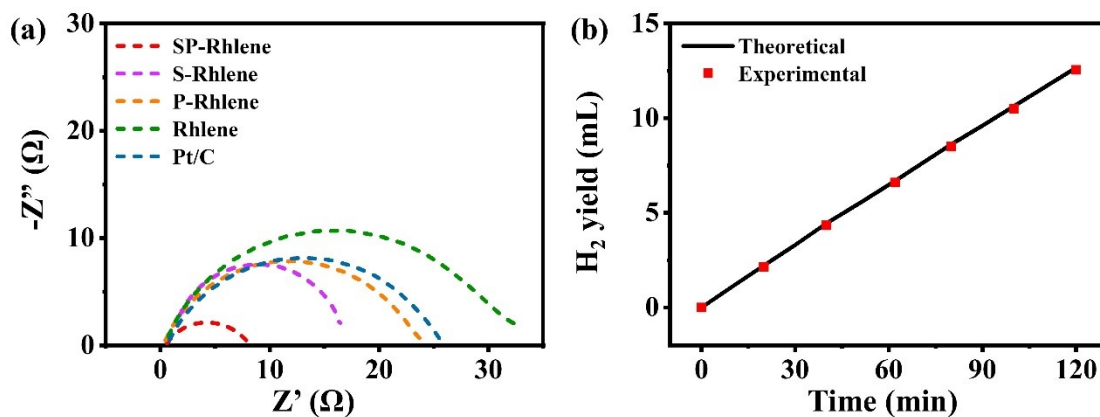


Fig. S11 (a) Nyquist plots for various electrocatalysts in 1 M KOH. (b) FE for H₂ production over SP-Rhylene with an overpotential of 970 mV.

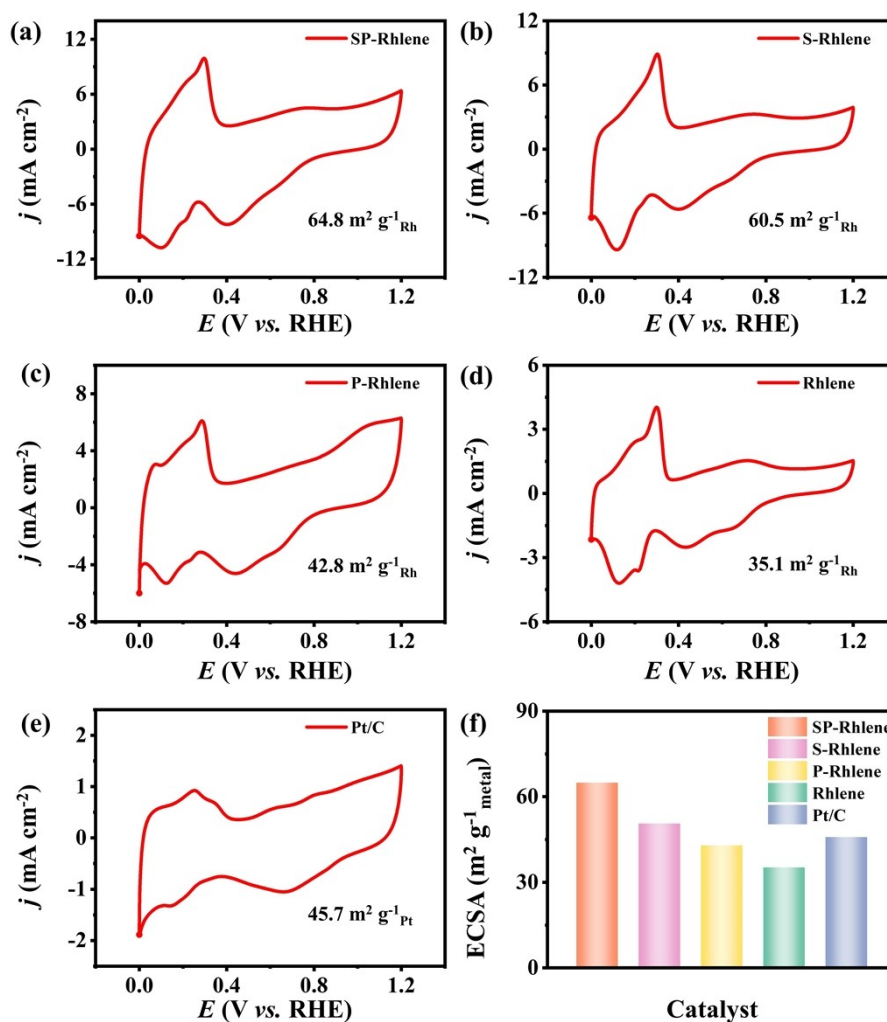


Fig. S12 CVs of the (a) SP-Rhylene, (b) S-Rhylene, (c) P-Rhylene, (d) Rhylene, and (e) Pt/C in a 1 M KOH solution with a scan rate of 50 mV s⁻¹. (f) The corresponding ECSAs.

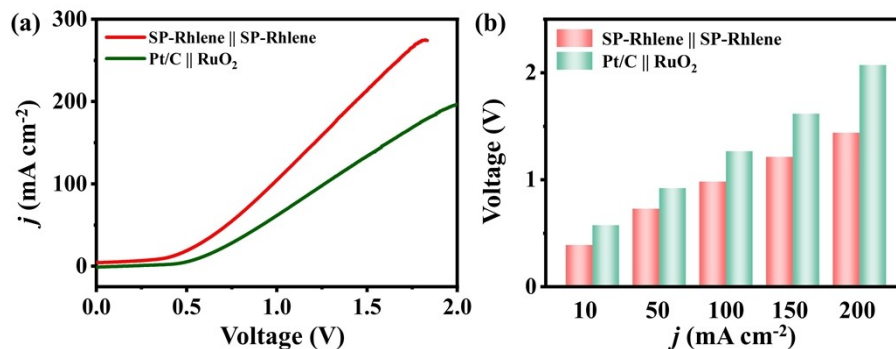


Fig. S13 (a) LSV curves of the SP-Rhylene || SP-Rhylene system and Pt/C || RuO₂ system and (b) the comparison voltages of different current densities.

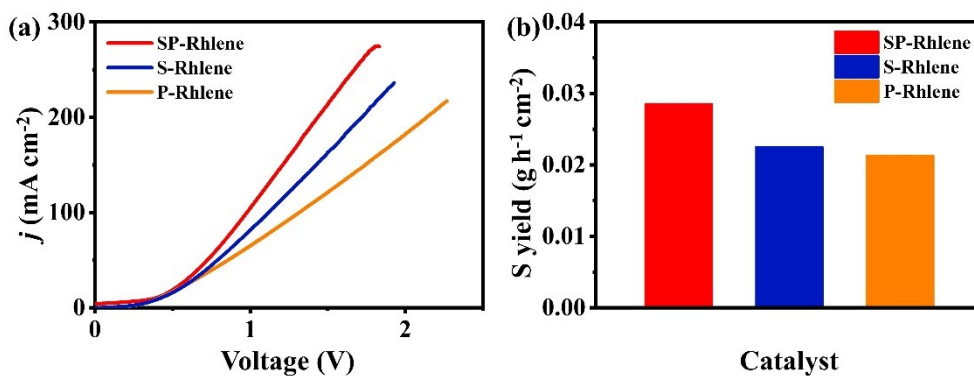


Fig. S14 (a) LSV curves of the SOR-HER system and (b) the S powder yield rates of the SP-Rhylene, S-Rhylene and P-Rhylene based on Chronoamperometric testing at 0.8 V for 24 h.